Science Arts & Métiers (SAM)

is an open access repository that collects the work of Arts et Métiers Institute of Technology researchers and makes it freely available over the web where possible.

This is an author-deposited version published in: https://sam.ensam.eu
Handle ID: .http://hdl.handle.net/10985/8662

To cite this version :

Didier CHICOT, Eli-Saul PUCHI-CABRERA, Alain IOST, M.H STAIA, Xavier DECOOPMAN, F. ROUDET, G. LOUIS - Analysis of indentation size effect in copper and its alloys - Materials Science and Technology - Vol. 29, n°7, p.868-876 - 2013

Any correspondence concerning this service should be sent to the repository Administrator : scienceouverte@ensam.eu

Arts et Métiers Institute of Technology

Analysis of indentation size effect in copper and its alloys

D. Chicot*[1], E. S. Puchi-Cabrera[1,2,3], A. Iost[1,4], M. H. Staia[2], X. Decoopman[1], F. Roudet[1] and G. Louis[1,5]

For describing the indentation size effect (ISE), numerous models, which relate the load or hardness to the indent dimensions, have been proposed. Unfortunately, it is still difficult to associate the different parameters involved in such relationships with physical or mechanical properties of the material. This is an unsolved problem since the ISE can be associated with various causes such as workhardening, roughness, piling-up, sinking-in, indenter tip geometry, surface energy, varying composition and crystal anisotropy. For interpreting the change in hardness with indent size, an original approach is proposed on the basis of composite hardness modelling together with the use of a simple model, which allows the determination of the hardness–depth profile. Applied to copper and copper alloys, it is shown that it is possible to determine the maximum hardness value reached at the outer surface of the material and the distance over which both the ISE and the workhardening take place.

Keywords: Hardness, Nanoindentation, Microindentation, Indentation size effect, Workhardening

Introduction

The indentation size effect (ISE) is an important problem for characterising the hardness of a material, intrinsic to the historical origin of indentation testing itself, as indicated by Walley in a recent review.[1] This phenomenon, which represents the dependence of hardness on the indent size, hinders the use of just a single parameter for an appropriate definition of hardness. For this reason, it is recognised in general that two parameters are required. One is the macrohardness, which corresponds to the hardness obtained by the application of an infinite load. The second one is an ISE parameter, which describes the extent of the hardness–indent size variation. Although there is an overall agreement among authors regarding the definition of the macrohardness, the expression of the ISE parameter is still a matter of discussion. The above observation has given rise to the existence of many relationships, which have been summarised and discussed in a review paper by Cheng and Cheng.[2] Among these relationships, some of them associate the applied load with the indent dimensions.[3–7] The other relationships express the hardness value as a function of the indent dimensions, which can be either the indent diagonal or the indentation depth, depending on the use of classical or instrumented indentation experiments respectively. Within this scope, the model of Nix and Gao,[8] based on the strain gradient plasticity (SGP) theory, is probably one of the most widely used ISE models, since it has the advantage of relating the two interdependent ISE parameters to intrinsic properties of the material.

As has been pointed out by Mokios and Aifantis,[9] during micro- and nanoindentation, sharp strain gradients develop near the indenter's tip, particularly for small to moderate indentation depths, which should be taken into account for the interpretation of related measurements of hardness versus indentation characteristics, such as penetration depth, contact radius and plastic zone size. The approach followed by Nix and Gao[8] to comply with this observation is based on Ashby's concept of geometrically necessary dislocations, whose density is directly related to plastic strain gradient. However, the analysis could also be conducted on the basis of a gradient plasticity formulation, as that advanced by Aifantis and co-workers,[10–12] which, in conjunction with Johnson's cavity model,[13] represents a valuable tool for interpreting the ISE. As indicated by Mokios and Aifantis,[9] for very small indentation depths, the observed ISE effect could be interpreted through gradient elasticity considerations, since plastic flow would not occur until the equivalent strain, in the gradient elasticity region surrounding the hydrostatically pressurised core beneath the indenter's tip, reached a critical yield value. In a recent communication, Zhao and co-workers[14] analysed the mechanism of dislocation nucleation from a surface in contact with a rigid wedge

indenter. These authors were able to propose a dislocation nucleation criterion for a surface loaded in contact, from which it was possible to estimate the critical contact size and dislocation emission angles for different wedge indenter apex angles.

Nevertheless, one important problem regarding the ISE analysis which remains to be solved is the determination of the physical meaning that the ISE parameters have. Thus, the ISE has been associated with various causes such as workhardening, roughness, piling-up, sinking-in, indenter tip geometry, surface energy, varying composition and crystal anisotropy. In addition, it can be dependent on the indentation conditions, like the zero determination of the load–displacement curve.[15] At nanoindentation scales, Soer *et al.*,[16] from the analysis of yield excursions present on the load–depth curves of bcc metals, have been able to show the existence of new types of ISE phenomena, which become apparent as the indenter approaches a grain boundary. In addition, it has been reported in the literature that the microhardness of different materials could be independent of load,[17,18] that it could increase or decrease with load[19–25] or that it could exhibit a complex variation with changes in load,[26–28] which makes very difficult the ISE analysis due to the variety of changes, especially in nanoindentation.[17,29–33]

However, after analysing the different models proposed for describing the ISE, it can be concluded that none of them is able to provide information regarding the distance from the surface after which no ISE occurs. This observation allows the association of the ISE phenomenon with a structural modification of the outer surface of the material, called 'hardened layer' or 'deformed zone' in the forthcoming, which is assumed to have a finite thickness. Thus, in the present work the application of different models originally developed for determining the hardness of thin films deposited onto a substrate is proposed. Under these conditions, the 'substrate' core is considered to have a constant hardness value equal to the macrohardness. This parameter would represent the hardness of the material prior to indentation, whereas the 'film' would be associated to the hardened layer. It is important to note that both the ISE and workhardening lead to an increase in hardness close to the material surface, two different phenomena which are difficult to model separately. Thus, it is possible that such a surface modification does not lead exactly to the superposition of two distinct materials having each a constant hardness, like in the case of a homogeneous hard film deposited onto a softer substrate. For this reason, the application of a simple model which allows the determination of the hardness–depth profile from hardness measurements performed normal to the material surface, aimed at determining the depth along which the hardness varies, is also attempted. The analysis of a load–depth curve obtained by instrumented microindentation leading to a continuous ISE analysis is also proposed, together with a detailed procedure for obtaining suitable indentation depth data. The investigation has been conducted on copper, brass and bronze, all of which exhibit workhardening during plastic deformation at room temperature.

Experimental techniques

Instrumented indentation experiments were performed employing a microhardness Tester CSM 2-107 equipped with a Vickers indenter. The load range of the instrument varies from 0·05 to 30 N. The load resolution is given for 100 μN and the depth resolution for 0·3 nm, these values being provided by the CSM Instruments Group. In this work, the maximum loads were chosen within the range 0·1–10 N and more than 20 indentation tests were performed. The values of the loading and unloading rates (expressed in mN min^{-1}) were set at twice the value of the maximum applied load, according to the rule proposed by Quinn *et al.*[34] A dwell time of 15 s was imposed according to the standard indentation test procedure ASTM E92 and E384-10e2.

Before the analysis of a load–depth curve, the experimental system was calibrated by performing indentations on fused silica for determining the contact stiffness of the instrument. In a second step, the computation of the frame compliance of the hardness tester is also required, which is subsequently introduced as a constant value into the numerical analysis of the indentation data. This is generally performed by following the correction proposed by Fischer-Cripps,[35] who considers that the experimental depth measurement includes part of the instrument elastic deformation. The magnitude of this correction is given by the product of the representative compliance term or frame compliance C_f and the load L, subtracted from the depth recorded by the instrument.

The methodologies advanced by Chicot *et al.*[36] based on the methodology proposed by Oliver and Pharr[37] can be employed for determining the C_f value, by means of an expression that relates the inverse of the contact stiffness $1/S$, with a function of the square root of the reciprocal contact area $1/A_C$, of the form

$$\frac{1}{S}=\left(\frac{\mathrm{d}h}{\mathrm{d}P}\right)_{h=h_m}=C_f+\frac{1}{2(\beta\gamma)E_R}\left(\frac{\pi}{A_C}\right)^{1/2}$$
$$\text{with } E_R=\left(\frac{1-\nu_m^2}{E_m}+\frac{1-\nu_i^2}{E_i}\right)^{-1} \quad (1)$$

In the above equation, E_R represents the reduced modulus, expressed as a function of E_m, E_i, ν_m and ν_i, which in turn represent the elastic modulus and the Poisson's ratio of the material and of the indenter, respectively. β and γ represent corrective factors introduced by Antunes *et al.*[38] and Hay *et al.*,[39] which allow the consideration of the Vickers indenter geometry, as well as the appropriate estimation of the radial displacement in the contact zone. For a diamond indenter, E_i=1140 GPa and ν_i=0·07.[40] Thus, by plotting the inverse of the contact stiffness ($1/S$) as a function of the square root of the reciprocal contact area $1/(A_C)^{1/2}$, a straight line is obtained, from which C_f can be readily obtained.

It is acknowledged that the rounded indenter tip has a significant influence on the determination of the contact area, especially for the lowest indentation depth values. Thus, in the present work, the correction suggested by Gong *et al.*[41] and Troyon and Huang[42] is employed, which consists in adding the measured indentation depth to the corrected depth, corresponding to the defect dimension of the indenter. A detailed analysis of the correction procedure has been published elsewhere.[36,43] The expression for the contact area derived from such a model, which also considers the indenter tip effect, is given as

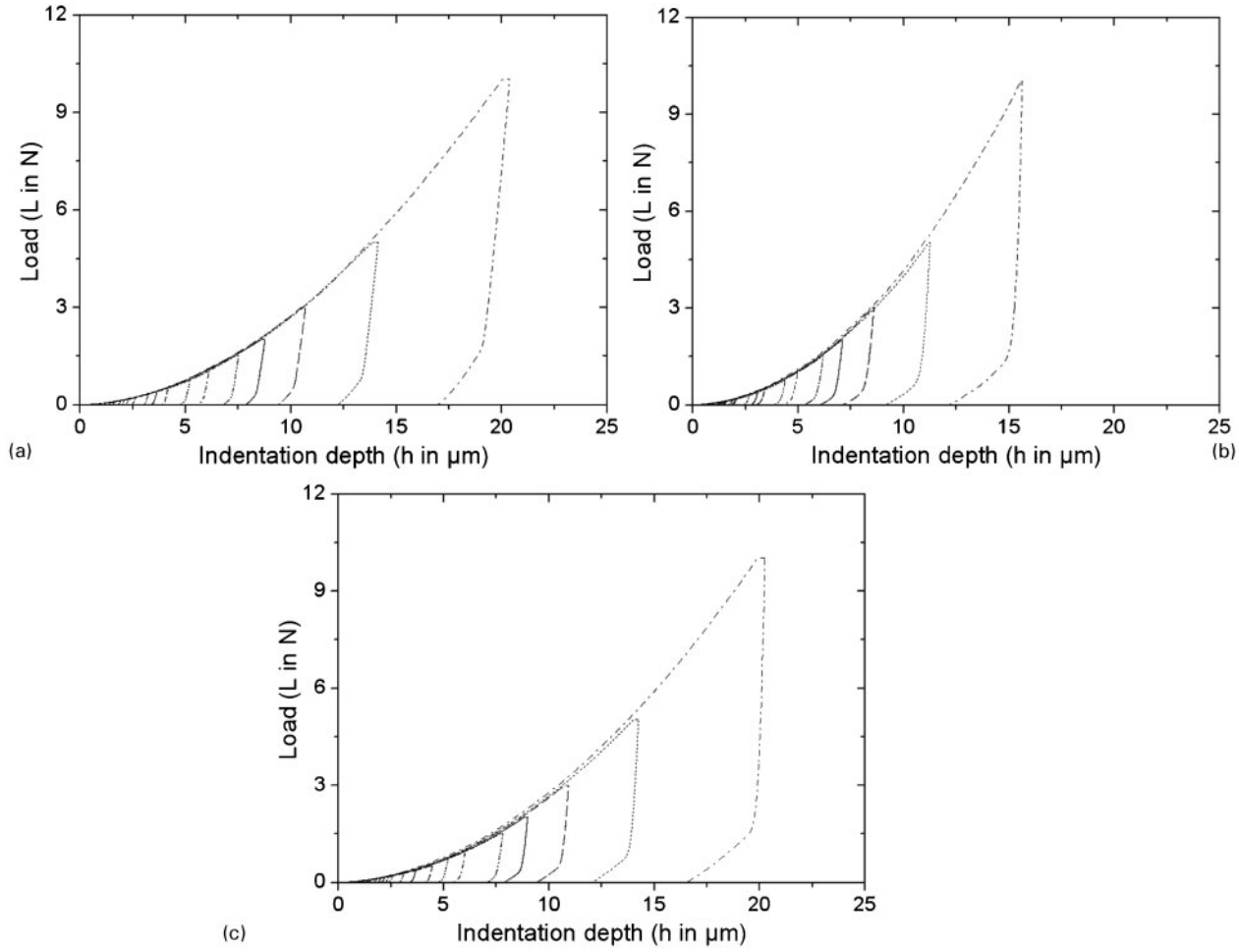

1 Load–depth curves obtained on *a* copper, *b* bronze and *c* brass with different applied loads ranging between 0·1 and 10 N

$$A_C = 24.5(h_C + h_{blunt})^2 \text{ instead of}$$
$$A_C = 24.5\,h_C^2 \text{ given by the instrument} \quad (2)$$

where h_C represents the contact indentation depth calculated from the unloading part of the load–depth curve and h_{blunt} represents the corrected depth corresponding to the defect dimension of the indenter. In this work, h_{blunt}=60 nm. In the presence of sinking-in, h_C is calculated following the methodology of Oliver and Pharr[37] whereas the methodology of Hochstetter *et al.*[44] is more appropriate when piling-up is generated around the indent.

In the present work, the hardness–indent size dependence has been studied using the Martens hardness, which can be computed over the entire loading curve by considering the continuous values of the applied load L_i and of the corrected indentation depth h_i. Accordingly

$$HM = \frac{L_i}{26{\cdot}43h_i^2} \quad (3)$$

In this investigation, the ISE of three common FCC materials has been studied: copper of 99% purity, a SAE 660 bronze and a 63/37 C27200 brass. The instrumented indentation experiments were performed on samples machined employing an abrasive saw. The specimens were ground using SiC papers of various grit sizes and subsequently polished using a series of diamond pastes having decreasing diamond grit size until 1 μm.

Experimental results and discussion

ISE modelling

Figure 1 illustrates the indentation load–depth curves for the tested materials and the satisfactory reproducibility of the indentation measurements, which were performed at different locations on the surface of the samples. As can be clearly observed in this figure, all the loading curves seem to superimpose quite well. For copper and its alloys, deformation around the indent is usually characterised by the formation of piling-up. Under these conditions, the model advanced by Hochstetter *et al.*[44] can be applied for determining the frame compliance by means of equation (1), which is afterwards used to correct the indentation displacement for an accurate calculation of the Martens hardness using equation (3).

To analyse the ISE, the different mathematical models available in the literature can be divided in two broad groups. Group 1 embraces the so called polynomial laws, which relate the applied load to the indentation dimension. Group 2, on the other hand, includes the models based on the SGP theory. For this reason, the preliminary analysis of the load-depth curves have been carried out employing one representative model of each group among the most used, i.e. the model of Bull and Page[7] similar to the proportional specimen resistance model, for group 1, and the model of Nix and Gao[8] for group 2. In addition, this choice has been motivated by

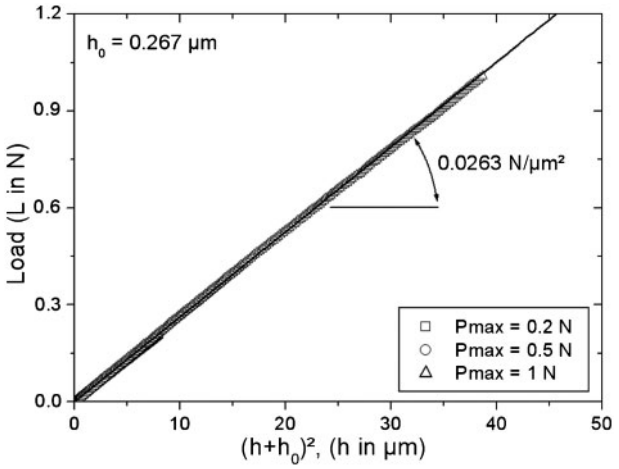

2 Model of Bull and Page[7] applied to indentation data obtained on copper sample

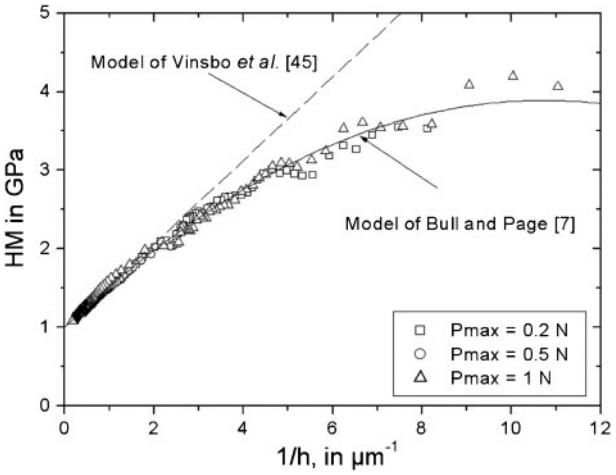

3 Results obtained with models of Bull and Page[7] and of Vingsbo *et al.*[45] applied to indentation data obtained on copper sample

the fact that these two models are often compared to each other.

The model of Bull and Page expresses the indentation load as a function of the indenter displacement by a second degree polynomial of the form

$$L = A_1(h+h_0)^2 \tag{4}$$

where A_1 and h_0 represent material constants.

Figure 2 illustrates the change in the applied load as a function of the indentation depth and the corresponding fitting curves resulting from the model of Bull and Page[7] applied to each loading curve obtained for the copper sample. It is clearly seen that this model accurately describes the change in indentation load with indentation depth regardless of the maximum load achieved. In order to incorporate the hardness indentation depth dependence into the Martens hardness calculation, as far as the model proposed by Bull and Page[7] is concerned, introduction of equation (4) into equation (3) leads to a second degree polynomial, as a function of the reciprocal indentation depth, expressed as

$$\mathrm{HM} = \frac{A_1}{26{\cdot}43}\frac{(h+h_0)^2}{h^2} = \frac{A_1}{26{\cdot}43} + \frac{2A_1h_0}{26{\cdot}43}\frac{1}{h} + \frac{A_1h_0^2}{26{\cdot}43}\frac{1}{h^2} \tag{5}$$

In the above expression, the term $A_1/26{\cdot}43$ can be considered as the macrohardness, HM_0. Moreover, the parameters A_1 and h_0 can be easily determined from the experimental data by least square analysis. This approach was employed for characterising the mechanical behaviour of the different materials analysed in the present investigation.

However, a much simpler relationship for describing the change in hardness with the inverse of the indentation depth consists in neglecting the second degree term in equation (5). This approach has been advanced by Vingsbo *et al.*,[45] who expressed the measured hardness simply as

$$H = H_0 + \frac{\Delta}{h} \tag{6}$$

where H_0 represents the macrohardness and Δ represents an ISE parameter.

Figure 3 represents the model of Vingsbo *et al.*[45] obtained for the copper sample and clearly illustrates that it is not adequate for representing the change in hardness, especially in the low indentation depth range. The above figure also shows that the best description is provided by a second degree polynomial. The results obtained for the model of Bull and Page[7] are summarised in Table 1, which presents the different ISE parameters for copper and its alloys. As a conclusion, the macrohardness values obtained for copper and brass are very similar and the ISE parameter can be interpreted in terms of size of deformation around the indent, according to the hypothesis advanced by Iost and Bigot.[46] However, such a parameter is not related to intrinsic properties of the tested materials.

On the contrary, one of the recent models proposed for the description of the ISE of crystalline materials, which undergo plastic deformation by dislocation slip, is that of Nix and Gao,[8] who introduced the concept of SGP based on dislocation theory principles. According to this model, the relationship between hardness and indentation depth can be expressed as

$$\frac{H}{H_0} = \left(1 + \frac{h^*_{\mathrm{NG}}}{h}\right)^{1/2} \tag{7}$$

where H_0 represents the macrohardness and h^*_{NG} is the characteristic scale length representing the ISE. Abu Al-Rub and Voyiadjis[47] have also developed a new method for determining a material length scale using microhardness results from conical or pyramidal indenters. The relation between the microhardness H, the macrohardness H_0, and their scale length parameter h^*_{AV} can be expressed as

$$\left(\frac{H}{H_0}\right)^{\beta} = 1 + \left(\frac{h^*_{\mathrm{AV}}}{h}\right)^{\beta/2} \tag{8}$$

Table 1 Values of ISE parameters deduced from Bull and Page[7] model applied to copper, bronze and brass samples

Materials	Copper	Bronze	Brass
A_1/N µm^{-2}	0·0263	0·0379	0·0253
h_0/µm	0·267	0·196	0·304
HM_0/GPa	1·00	1·43	0·96

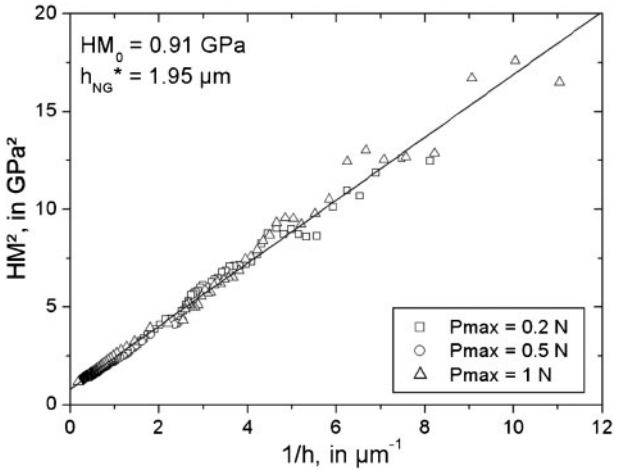

4 Results obtained with model of Nix and Gao[8] applied to indentation data obtained on copper sample

It can be observed that by setting $\beta=2$ in equation (8), equation (7) is readily obtained.

In the case of this latter model, since the exponent β is restricted to vary in the interval $1\leq\beta\leq2$, it has to be determined by means of constrained optimisation techniques. Thus, as expected for the type of materials under investigation, a value of $\beta=2$ has been obtained, in agreement with the model advanced by Nix and Gao.[8] For this reason, Fig. 4 only represents the results derived from the Nix and Gao model[8] applied to the experimental results obtained from the copper sample. As a result, a value of 0·91 GPa has been determined for the macrohardness, which is close to the value of 1 GPa obtained by means of the model of Bull and Page.[7] The results obtained by means of Nix and Gao model[8] for copper and its alloys are summarised in Table 2. It is noticeable that the macrohardness values that have been determined are similar to those obtained by means of the Bull and Page[7] model (Table 1). Concerning the characteristic scale length, it is difficult to associate its value to a geometrical feature of the deformed material. Nevertheless, the values summarised in Table 2 are of the same order of magnitude of the characteristic scale lengths obtained for different materials, whose values have been reported elsewhere.[48]

As a conclusion, it is clear that the model of Vingsbo *et al.*[45] is not appropriate for describing the ISE since the equation (6) is in contradiction with equation (7) due to Nix and Gao.[8] However, when considering equation (5) of Bull and Page[7] and the approximation resulting from a Taylor expansion of the square root function, the two equations can be compared. A preliminary analysis shows that the ratio between h^*_{NG} of Nix and Gao[8] and h_0 of Bull and Page[7] should be close to 4. Nevertheless, this is not exactly the case due to the mathematical approximations involved.

Table 2 Values of ISE parameters deduced from Nix and Gao[8] model applied to copper, bronze and brass samples

Materials		Copper	Bronze	Brass
Nix and Gao[8]	HM_0/GPa	0·91	1·48	0·70
	h^*_{NG}/μm	1·95	0·71	4·32

Use of composite hardness models

Whatever the ISE model used, regardless if some of them are able to relate the ISE parameters to intrinsic material properties, it is not possible to have information concerning the hardness reached at the outer surface of the material or the distance along which the hardness varies. For this reason, the application of different models devoted originally to the mechanical characterisation of coated systems has been suggested. However, the original models have to be modified in order to take into account the fact that the thickness of the hardened layer is not known before the indentation data analysis.

Three of the models that can be employed for this purpose, mainly for their simplicity, are those earlier advanced by Jönsson and Hogmark,[49] Korsunsky *et al.*[50] and Puchi-Cabrera.[51,52] These models assume the validity of a linear law of mixtures for expressing the composite hardness as a function of the film and substrate hardness. The main difference between them arises from the definition of the volume fraction of coating that contributes to the measured hardness. In the case of the ISE analysis, the measured hardness H_C can be simply defined as

$$H_C = H_0 + a(H_{surf} - H_0) \tag{9}$$

where H_0 represents the macrohardness of the material before indentation, H_{surf} represents the hardness of the hardened layer or plastically deformed material close to the outer surface and 'a' represents the volume fraction, in this case, of the hardness layer that contributes to the measured hardness. Unfortunately, for the ISE analysis, it is not possible to determine *a priori* the hardened layer thickness. However, both this parameter and the indentation depth are implicitly involved in the coefficient 'a', whose definition depends on the particular model employed, as indicated above.

For example, the model advanced by Jönsson and Hogmark[49] considers the load supporting areas under the indent associated with the substrate and film. From geometrical considerations, these authors have expressed the film volume fraction which contributes to the composite hardness by means of the following relationship

$$a = 2\left(\frac{C}{h}\right) - \left(\frac{C}{h}\right)^2 \tag{10}$$

where C, expressed in μm, represents a constant, which could take different values depending on the nature of the indented material. According to this model and for a Vickers indenter, C is equal to $0{\cdot}1428t$ for ductile materials and $0{\cdot}0714t$ for brittle materials, where t represents the thickness of the film or, as in the present case, the thickness of the surface hardened layer.

A disadvantage of this model, generally reported in the literature, is that due to its particular definition, the parameter 'a' could attain values greater than 1 at low indentation depths, depending on the magnitude of the parameter C. Obviously, if $a>1$, the contact area between the indenter and the coating is negative, which does not have any physical meaning. As reported by Iost and Bigot[53] and Guillemot *et al.*[54] the application of this model to the description of the composite hardness as a function of the indentation depth requires some cautions

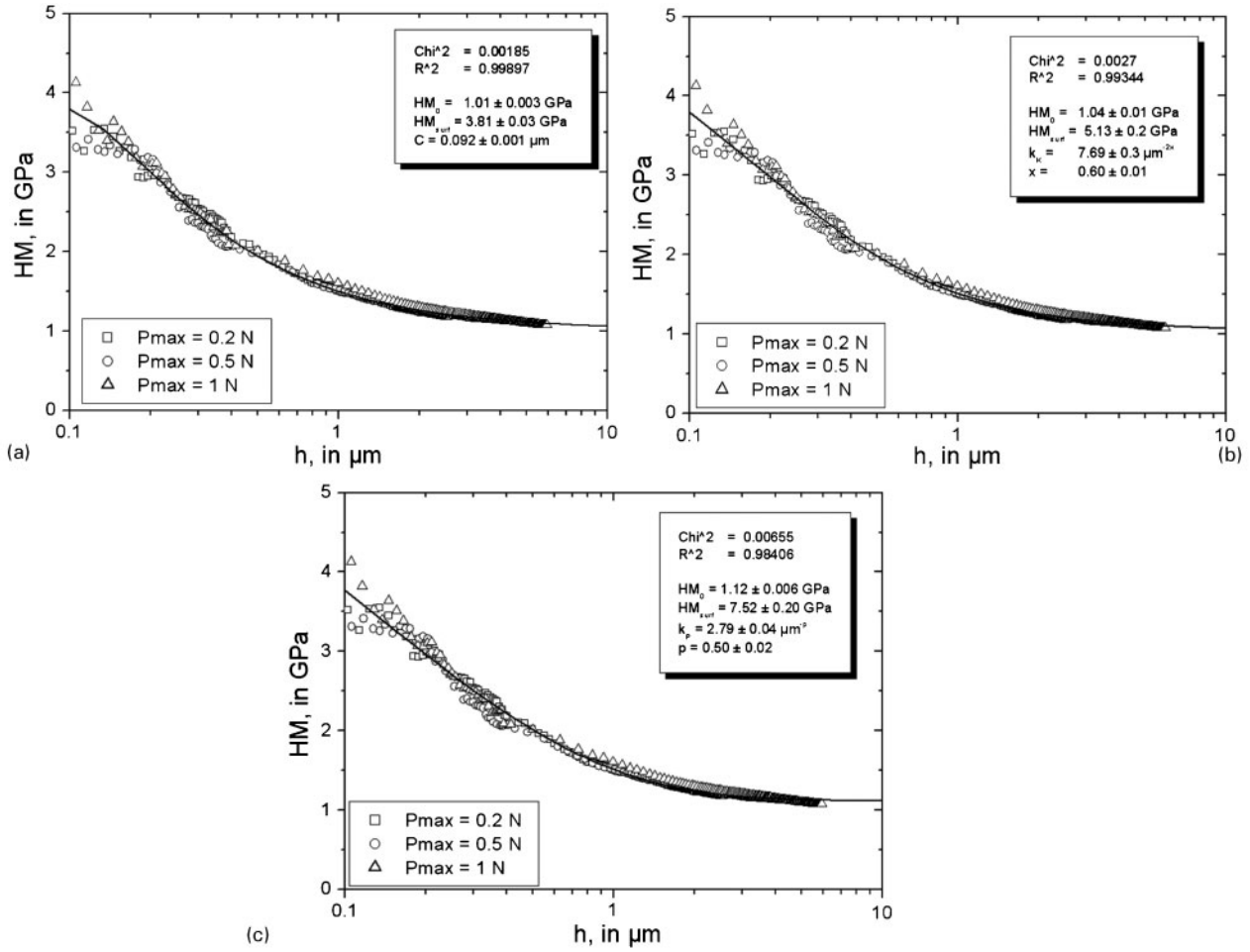

a Jönsson and Hogmark[49] model; *b* Korsunsky *et al.*[50] model; *c* Puchi-Cabrera[51,52] model

5 Composite hardness models applied to indentation data obtained for copper sample

since the variation of 'a' has to be restricted to the interval $0 \leq a \leq 1$. Thus, equation (10) can be applied only if $h \leq C$, condition that defines the limiting value of the penetration depth for which the coating influences the measured hardness. On the contrary, an advantage of this model is that it allows the determination of an equivalent thickness of the hardened layer t, due to the proportionality between the latter and the parameter C.

Korsunsky *et al.*[50] developed an alternative model based on the work of indentation associated with the deformation energy of the two materials and their interface under the indent. In the original model, the parameter 'a' is given by

$$a = \frac{1}{1 + k_K h^2} \tag{11}$$

However, this model has been generalised by Tuck *et al.*[55] giving the possibility that the exponent of the indentation depth could take different values other than 2. According to this generalised model, the coefficient, 'a', is expressed as

$$a = \frac{1}{1 + k_K h^{2x}} \tag{12}$$

However, the parameter k_K can be rewritten in terms of the hardened layer thickness as k'_K/t, where k'_K represents the original coefficient introduced by Korsunsky *et al.*[50]

Puchi-Cabrera[51,52] also proposed the computation of the composite hardness by considering that the volume fraction of coating is given by

$$a = \exp\left(-k_P h^P\right) \tag{13}$$

where the two constants, k_P and p, represent material parameters which are determined from the experimental data. In this relation, the coefficient k_P involves the film thickness, since it can be expressed as $k_P = k'_P/t^P$ where k'_P is the original coefficient proposed by Puchi-Cabrera.[51,52]

Contrary to the model proposed by Jönsson and Hogmark,[49] in the models advanced by Korsunsky *et al.*[50] and Puchi-Cabrera,[51,52] as shown in equations (12) and (13), the volume fraction of coating that contributes to the composite hardness is limited to the interval $0 \leq a \leq 1$ and therefore, these approaches can be used confidently in the whole range of indentation depths.

Figure 5 illustrates the application of these three models to the copper sample. On each figure, the values corresponding to the macrohardness HM_0, the hardness reached at the outer surface HM_{surf} and the different ISE parameters depending on the applied model have been given. From a general point of view, the three models are observed to provide a satisfactory description of the hardness–indentation depth change.

Table 3 summarises the different ISE parameters resulting from the application of the different composite

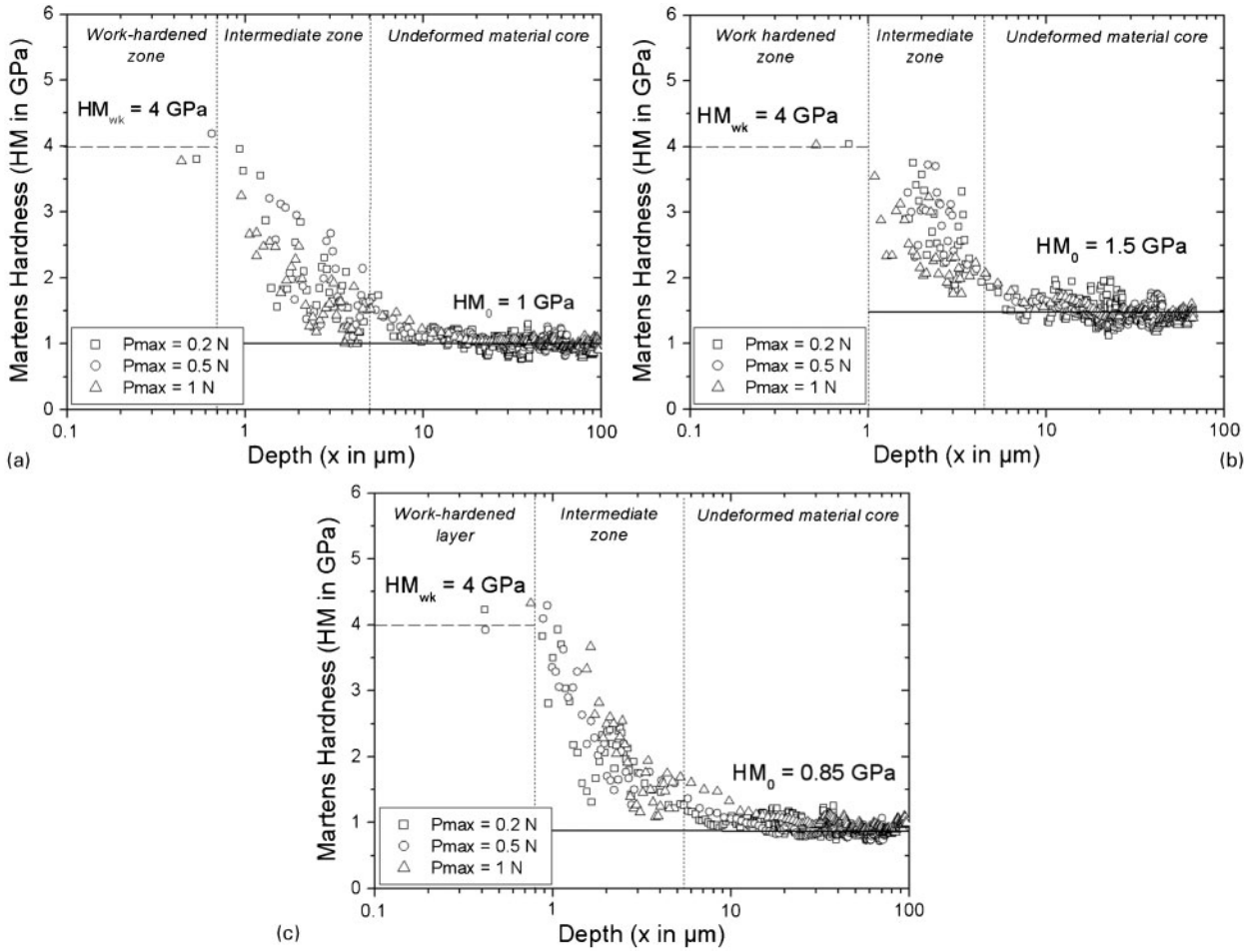

6 Hardness–depth profile modelling applied to ISE analysis of *a* copper, *b* bronze and *c* brass

hardness models. In addition, the relative hardness variation parameter has been computed, which indicates the extent of the ISE. The macrohardness values HM_0 derived from the application of these models are very similar. For the models of Jönsson and Hogmark[49] and Korsunsky *et al.*,[50] the computed values of the hardness at the outer surface are also very similar, whereas for the model of Puchi-Cabrera,[51,52] these are somewhat higher. Although the application of the composite hardness models seems to be very useful for determining the hardness value at the outer surface of the material, it also seems unsuitable for describing accurately the ISE by means of the parameters k_K and k_P involved in the Korsunsky *et al.*[50] and Puchi-Cabrera[51,52] models, possibly due to their dependence on the hardened surface layer thickness.

However, the two exponents x and p involved into these two models seem to be interesting, since their values increase following the same trend, independently of the tested materials. Nevertheless, additional ISE analyses of various massive materials are required to establish the appropriate meaning of these parameters. On the other hand, the constant C involved in the Jönsson and Hogmark[49] model, allows the determination of an equivalent thickness of the hardened layer since this constant is equal to $0{\cdot}1428t$ for ductile materials without crack formation during the indentation process, which is the case of the tested alloys.

According to this relation, the equivalent thickness of the deformed zone, considered as the hardened layer, is equal to 0·63 μm for copper, 1·05 μm for bronze and 0·84 μm for brass. The latter value agrees very well with the results reported by Samuels[56] who found that the deformation depth, i.e. the maximum depth from the root of surface scratches to the elastic/plastic boundary, is equal to 0·7 μm for a 70 : 30 brass polished using a 1 μm diamond paste.

Table 3 Values of ISE parameters derived from composite hardness models of Jönsson and Hogmark,[49] Korsunsky *et al.*[50] and Puchi-Cabrera[51,52] applied to copper, bronze and brass samples

Materials		Copper	Bronze	Brass
Jönsson and Hogmark[49]	HM_0/GPa	1·02	1·46	0·85
	HM_{surf}/GPa	3·81	3·29	3·97
	C	0·09	0·15	0·12
Korsunsky *et al.*[50]	HM_0/GPa	1·04	1·47	0·94
	HM_{surf}/GPa	5·13	3·81	4·32
	k_K	7·69	3·32	4·29
	x	0·60	0·65	0·74
Puchi-Cabrera[51,52]	HM_0/GPa	1·12	1·55	1·02
	HM_{surf}/GPa	7·52	4·91	5·27
	k_P	2·79	1·94	1·98
	p	0·50	0·60	0·72

Hardness–depth profile modelling

In a previous investigation,[43] a simple hardness model, which allowed the determination of the microhardness–depth profile from a load–depth curve in a nitrocarburised

Analysis of indentation size effect in copper and its alloys

D. Chicot*[1], E. S. Puchi-Cabrera[1,2,3], A. Iost[1,4], M. H. Staia[2], X. Decoopman[1], F. Roudet[1] and G. Louis[1,5]

For describing the indentation size effect (ISE), numerous models, which relate the load or hardness to the indent dimensions, have been proposed. Unfortunately, it is still difficult to associate the different parameters involved in such relationships with physical or mechanical properties of the material. This is an unsolved problem since the ISE can be associated with various causes such as workhardening, roughness, piling-up, sinking-in, indenter tip geometry, surface energy, varying composition and crystal anisotropy. For interpreting the change in hardness with indent size, an original approach is proposed on the basis of composite hardness modelling together with the use of a simple model, which allows the determination of the hardness–depth profile. Applied to copper and copper alloys, it is shown that it is possible to determine the maximum hardness value reached at the outer surface of the material and the distance over which both the ISE and the workhardening take place.

Keywords: Hardness, Nanoindentation, Microindentation, Indentation size effect, Workhardening

Introduction

The indentation size effect (ISE) is an important problem for characterising the hardness of a material, intrinsic to the historical origin of indentation testing itself, as indicated by Walley in a recent review.[1] This phenomenon, which represents the dependence of hardness on the indent size, hinders the use of just a single parameter for an appropriate definition of hardness. For this reason, it is recognised in general that two parameters are required. One is the macrohardness, which corresponds to the hardness obtained by the application of an infinite load. The second one is an ISE parameter, which describes the extent of the hardness–indent size variation. Although there is an overall agreement among authors regarding the definition of the macrohardness, the expression of the ISE parameter is still a matter of discussion. The above observation has given rise to the existence of many relationships, which have been summarised and discussed in a review paper by Cheng and Cheng.[2] Among these relationships, some of them associate the applied load with the indent dimensions.[3–7] The other relationships express the hardness value as a function of the indent dimensions, which can be either the indent diagonal or the indentation depth, depending on the use of classical or instrumented indentation experiments respectively. Within this scope, the model of Nix and Gao,[8] based on the strain gradient plasticity (SGP) theory, is probably one of the most widely used ISE models, since it has the advantage of relating the two interdependent ISE parameters to intrinsic properties of the material.

As has been pointed out by Mokios and Aifantis,[9] during micro- and nanoindentation, sharp strain gradients develop near the indenter's tip, particularly for small to moderate indentation depths, which should be taken into account for the interpretation of related measurements of hardness versus indentation characteristics, such as penetration depth, contact radius and plastic zone size. The approach followed by Nix and Gao[8] to comply with this observation is based on Ashby's concept of geometrically necessary dislocations, whose density is directly related to plastic strain gradient. However, the analysis could also be conducted on the basis of a gradient plasticity formulation, as that advanced by Aifantis and co-workers,[10–12] which, in conjunction with Johnson's cavity model,[13] represents a valuable tool for interpreting the ISE. As indicated by Mokios and Aifantis,[9] for very small indentation depths, the observed ISE effect could be interpreted through gradient elasticity considerations, since plastic flow would not occur until the equivalent strain, in the gradient elasticity region surrounding the hydrostatically pressurised core beneath the indenter's tip, reached a critical yield value. In a recent communication, Zhao and co-workers[14] analysed the mechanism of dislocation nucleation from a surface in contact with a rigid wedge

[1]Université Lille Nord de France, USTL, LML, CNRS, UMR 8107, F-59650 Villeneuve d'Ascq, France
[2]School of Metallurgical Engineering and Materials Science, Faculty of Engineering, Universidad Central de Venezuela, Postal Address 47885, Los Chaguaramos, Caracas, 1041, Venezuela
[3]Venezuelan National Academy for Engineering and Habitat, Palacio de las Academias, Postal Address 1723, Caracas 1010, Venezuela
[4]Arts et Métiers ParisTech – Centre de Lille, 8, Boulevard Louis XIV, 59000 Lille Cedex, France
[5]EMDouai, MPE-GCE, F-59500 Douai, France

*Corresponding author, email didier.chicot@univ-lille1.fr

© 2013 Institute of Materials, Minerals and Mining
Published by Maney on behalf of the Institute
Received 3 December 2012; accepted 21 January 2013
DOI 10.1179/1743284713Y.0000000213

11. I. Tsagrakis, A. Konstantinidis and E. C. Aifantis: 'Strain gradient and wavelet interpretation of size effects in yield and strength', *Mech. Mater.*, 2003, **35**, 733–745.
12. E. C. Aifantis: 'Gradient plasticity', in 'Handbook of materials behavior models', (ed. J. Lemaitre), 291–307; 2001, New York, Academic Press.
13. K. L. Johnson: 'The correlation of indentation experiments', *J. Mech. Phys. Solids*, 1970, **18**, 115–126.
14. J. Zhao, L. F. Ma and A. M. Korsunsky: 'Surface dislocation nucleation by wedge indenter contacts', *Mater. Sci. Technol*., 2012, **28**, 1167–1172.
15. M. Bigerelle, P. E. Mazeran and M. Rachik: 'The first indenter-sample contact and the indentation size effect in nano-hardness measurement', *Mater. Sci. Eng. C*, 2007, **C27**, 1448–1451.
16. W. A. Soer, K. E. Aifantis and J. Th. M. de Hosson: 'Incipient plasticity during nanoindentation at grain boundaries in body-centered cubic metals', *Acta Mater.*, 2005, **53**, 4665–4676.
17. C. Ascheron, C. Huse, G. Kuhn and H. Neumann: 'Microhardness of Sn-doped InP', *Cryst. Res. Technol.*, 1989, **24**, 33–35.
18. D. W. Johnson, E. M. Vogel and B. B. Hate: Proc. 3rd Int. Conf. on 'Ferrites', (ed. H. Watanabe), 285; 1980, Tokyo, Centre for Academic Publications.
19. B. Vengatesan, H. Kanniah and P. Ramasamy: 'Microhardness and crack patterns of CVT grown $CdGa_2S_4$ single crystals', *J. Mater. Sci. Lett.*, 1986, **5**, 987–988.
20. P. N. Kotru, A. K. Razdan and B. M. Wanklyn: 'Microhardness of flux grown pure doped and mixed rare earth aluminates and orthochromites', *J. Mater. Sci.*, 1989, **24**, 793–803.
21. K. Balakrishnan, B. Vengatesan, H. Kanniah and P. Ramasamy: 'Growth and microindentation studies of $CulnSe_2$ single crystals', *J. Mater. Sci. Lett*., 1990, **9**, 785–787.
22. M. R. Sridhar and M. M. Yovanovich: 'Empirical methods to predict Vickers microhardness', *Wear*, 1996, **193**, 91–98.
23. K. Bamzai, P. N. Kotru and B. M. Wanklyn: 'Hardness studies and fracture behaviour on flux-grown $YFeO_3$ single crystals', *Cryst. Res. Technol.*, 1996, **31**, 813–819.
24. R. Tickoo, R. P. Tandon, K. K. Bamzai and P. N. Kotru: 'Microindentation studies on samarium-modified lead titanate ceramics', *Mater. Chem. Phys*., 2003, **80**, 446–451.
25. B. Zhang, W. Wang and G. P. Zhang: 'Depth dependent hardness variation in Ni–P amorphous film under nanoindentation', *Mater. Sci. Technol*., 2006, **22**, 734–737.
26. V. P. Bhatt, R. M. Patel and C. F. Desai: 'Deformation and microhardness studies on $KCPO_4$ single crystals', *Cryst. Res. Technol.*, 1983, **18**, 1173–1179.
27. J. Guille and M. Sieskind: 'Microindentation studies on BaFCl single crystals', *J. Mater. Sci.*, 1991, **26**, 899–903.
28. P. R. Dhar, K. Bamzai and P. N. Kotru: 'Deformation and microhardness studies on natural apophyllite crystals', *Cryst. Res. Technol.*, 1997, **32**, 537–544.
29. K. E. Aifantis, W. A. Soer, J. Th. M. de Hosson and J. R. Willis: 'Interfaces within strain gradient plasticity: theory and experiments', *Acta Mater*., 2006, **54**, 5077–5085.
30. B. Yang and H. Vehoff: 'Dependence of nanohardness upon indentation size and grain size. A local examination of the interaction between dislocations and grain boundaries', *Acta Mater*., 2007, **55**, 849–856.
31. G. Z. Voyiadjis, A. H. Almasri and T. Park: 'Experimental nanoindentation of BCC metals', *Mech. Res. Commun*., 2010, **37**, 307–314.
32. G. Z. Voyiadjis, D. Faghihi and C. Zhang: 'Analytical and experimental determination of rate, and temperature dependent length scales', *J Nanomech. Micromech. ASCE*, 2011, **1**, 24–40.
33. D. Faghihi and G. Z. Voyiadjis: 'Determination of nanoindentation size effects and variable material intrinsic length scale for body-centered cubic metals', *Mech. Mater*., 2012, **44**, 189–211.
34. G. D. Quinn, P. L. Patel and I. Lloyd: 'Effect of loading rate upon conventional ceramic microindentation hardness', *J. Res. Natl. Inst. Stand. Technol.*, 2002, **107**, 299–306.
35. A. C. Fischer-Cripps: 'Critical review of analysis and interpretation of nano-indentation test data', *Surf. Coat. Technol*., 2006, **200**, 4153–4165.
36. D. Chicot, F. Roudet, A. Zaoui, G. Louis and V. Lepingle: 'Influence of visco-elasto-plastic properties of magnetite on the elastic modulus: multicyclic indentation and theoretical studies', *Mater. Chem. Phys*., 2010, **119**, 75–81.
37. W. C. Oliver and G. M. Pharr: 'An improved technique for determining hardness and elastic modulus using load and displacement sensing indentation experiments', *J. Mater. Res*., 1992, **7**, 1564–1583.
38. J. M. Antunes, L. F. Menezes and J. V. Fernandes: 'Three-dimensional numerical simulation of Vickers indentation tests', *Int. J. Sol. Struct*., 2006, **43**, 784–806.
39. J. C. Hay, A. Bolshakov and G. M. Pharr: 'Critical examination of the fundamental relations used in the analysis of nano-indentation data', *J. Mater. Res*., 1999, **14**, 2296–2305.
40. J. E. Field and R. H. Telling: 'The Young modulus and Poisson ratio of diamond', Research Note; 1999, Cambridge, Cavendish Laboratory.
41. J. Gong, H. Miao and Z. Peng: 'On the contact area for nanoindentation tests with Berkovich indenter: case study on soda-lime glass', *Mater. Lett*., 2004, **58**, 1349–1353.
42. M. Troyon and L. Huang: 'Correction factor for contact area in nanoindentation measurements', *J. Mater. Res*., 2005, **20**, 610–617.
43. D. Chicot, E. S. Puchi-Cabrera, X. Decoopman, F. Roudet, J. Lesage and M. H. Staia: 'Diamond-like carbon film deposited on nitrided 316L stainless steel substrate: a hardness depth-profile modeling', *Diamond Relat. Mater*., 2011, **20**, 1344–1352.
44. G. Hochstetter, A. Jimenez and J. L. Loubet: 'Strain-rate effects on hardness of glassy polymers in the nanoscale range. Comparison between quasi-static and continuous stiffness measurements', *J. Macromol. Sci.*, 1999, **B38**, 681–692.
45. O. Vingsbo, S. Hogmark, B. Jönsson and A. Ingemarsson: in 'Microindentation techniques in materials science and engineering', (ed. P. J. Blau and B. R. Lawn), ASTM STP 889, Chapter 15, 257–271; 1986, Philadelphia, PA, ASTM.
46. A. Iost and R. Bigot: 'Indentation size effect: reality or artefact?', *J. Mater. Sci*., 1996, **31**, 3573–3577.
47. R. K. Abu Al-Rub and G. Z. Voyiadjis: 'Analytical and experimental determination of the material intrinsic length scale of strain gradient plasticity theory from micro- and nano-indentation experiments', *Int. J. Plast*., 2004, **20**, 1139–1182.
48. D. Chicot: 'Hardness length-scale factor to model nano- and micro-indentation size effects', *Mater. Sci. Eng. A*, 2009, **A499**, 454–461.
49. B. Jönsson and S. Hogmark: 'Hardness measurements of thin films', *Thin Solid Films*, 1984, **114**, 257–269.
50. A. M. Korsunsky, M. R. McGurk, S. J. Bull and T. F. Page: 'On the hardness of coated systems', *Surf. Coat. Technol*., 1998, **99**, 171–183.
51. E. S. Puchi-Cabrera: 'A new model for the computation of the composite hardness of coated systems', *Surf. Coat. Technol*., 2002, **160**, 177–186.
52. E. S. Puchi-Cabrera: 'On the computation of the composite hardness of coated systems', *Surf. Eng*., 2004, **20**, 332–344.
53. A. Iost and R. Bigot': Hardness of coatings', *Surf. Coat. Technol*., 1996, **80**, 117–120.
54. G. Guillemot, A. Iost and D. Chicot: 'Comments on the paper ''Modification of composite hardness models to incorporate indentation size effects in thin films'', D. Beegan, S. Chowdhury and M.T. Laugier, Thin Solid Films 516 (2008), 3813–3817', *Thin Solid Films*, 2010, **518**, 2097–2101.
55. J. R. Tuck, A. M. Korsunsky, D. G. Bhat and S. J. Bull: 'Indentation hardness evaluation of cathodic arc deposited thin hard coatings', *Surf. Coat. Technol*., 2001, **139**, 63–74.
56. L. E. Samuels: 'Metallographic polishing by mechanical methods'; 1982, Metals Park, OH, ASM International.